RAPID COMMUNICATION

Strong spin frustration and magnetism in kagomé antiferromagnets LnCu$_3$(OH)$_6$Br$_3$ (Ln = Nd, Sm, and Eu)

Jin-Qun Zhong(钟金群)[1], Zhen-Wei Yu(余振伟)[1], Xiao-Yu Yue(岳小宇)[5], Yi-Yan Wang(王义炎)[2], Hui Liang(梁慧)[2], Yan Sun(孙燕)[2], Dan-Dan Wu(吴丹丹)[2], Zong-Ling Ding(丁宗玲)[4], Jin Sun(孙进)[4], Xue-Feng Sun(孙学峰)[3,‡], and Qiu-Ju Li(李秋菊)[4,†]

[1] *School of Materials Science and Engineering, Anhui University, Hefei* 230601, *China*
[2] *Institute of Physical Science and Information Technology, Anhui University, Hefei* 230601, *China*
[3] *Department of Physics, and Key Laboratory of Strongly-Coupled Quantum Matter Physics (CAS), University of Science and Technology of China, Hefei* 230026, *China*
[4] *School of Physics and Optoelectronic engineering, Anhui University, Hefei* 230601, *China*
[5] *School of Optical and Electronic Information, Suzhou City University, Suzhou* 215104, *China*

(Received 9 January 2023; revised manuscript received 3 February 2023; accepted manuscript online 8 February 2023)

To study the effects of lanthanide ions on the geometrically frustrated antiferromagnets and their magnetic properties, we grew high-quality single crystals of LnCu$_3$(OH)$_6$Br$_3$ (Ln = Nd, Sm, and Eu) by hydrothermal method and studied their crystal structures and magnetic properties. The refinements of the crystal structure referred to the powder x-ray diffraction data show that LnCu$_3$(OH)$_6$Br$_3$ adopt a Kapellasite-type layer structure, which is isostructural to their chlorine analogue. Magnetic susceptibilities demonstrate that LnCu$_3$(OH)$_6$Br$_3$ have strong antiferromagnetic coupling and a pronounced magnetic frustration effect. Magnetization measurements indicate canted antiferromagnetic ordering of Cu^{2+} ions around 16 K within the kagomé plane and weak ferromagnetic coupling. Moreover, shoulder-like anomalies in specific heat around 16 K could be a signature of emergent of magnetic ordering. The low-temperature negative magnetization and specific heat of LnCu$_3$(OH)$_6$Br$_3$ (Ln = Nd, Sm, and Eu) indicate that Ln^{3+} ions induce more exotic magnetic ground state properties.

Keywords: kagomé lattice, antiferromagnet, single crystal, spin frustration

PACS: 75.10.Jm, 75.40.Cx, 06.60.Ei, 61.05.cp **DOI:** 10.1088/1674-1056/acb9e8

1. Introduction

Geometrically frustrated antiferromagnetic systems with kagomé lattice have been the central topics for their exotic quantum spin liquid (QSL) state.[1–8] Many prominent $S = 1/2$ kagomé Heisenberg antiferromagnets, including ZnCu$_3$(OH)$_6$Cl$_2$, YCu$_3$(OH)$_6$Cl$_3$ and YCu$_3$(OH)$_6$Br$_2$[Br$_x$(OH)$_{1-x}$], have been proposed as the most promising candidates with the QSL ground state, which show no conventional magnetic phase transitions with temperature close to absolute zero despite of the strong exchange couplings.[9–21] Herbertsmithite ZnCu$_3$(OH)$_6$Cl$_2$ is the best candidate for a kagomé QSL in experimental investigations, although it still remains controversial on the ground state properties so far.[9–12] For Kapellasite structure YCu$_3$(OH)$_6$Cl$_3$ with a perfect kagomé lattice of Cu^{2+} ($S = 1/2$) ions, the coexistence of magnetic ordering and persistent spin dynamics at low temperatures is of particular.[14–16] Magnetic and muon spin relaxation measurements revealed that the magnetic ordering at low temperatures is unusual and its mechanism is a challenge for future theoretical and experimental studies.[15,16] Later, YCu$_3$(OH)$_6$Br$_2$[Br$_x$(OH)$_{1-x}$], with $(OH)^-$ group partially substituting the Br^- ions, has been successfully synthesized and reported as a kagomé QSL candidate, which exhibited no magnetic transition at low temperatures down to 50 mK despite of the strong antiferromagnetic coupling.[17–20] However, another study of YCu$_3$(OH)$_6$Br$_2$[Br$_x$(OH)$_{1-x}$] by theoretical and experimental investigations suggested that the bond randomness between $(OH)^-$ and Br^- ions is significant.[19]

In order to investigate the bulk magnetic properties of LnCu$_3$(OH)$_6$Br$_3$, we introduced trivalent Ln^{3+} (Ln = Nd, Sm, and Eu) ions to replace nomagnetic Y^{3+} ions of YCu$_3$(OH)$_6$Br$_3$ and grew high-quality single crystals of LnCu$_3$(OH)$_6$Br$_3$ using the hydrothermal method. The x-ray diffraction data of LnCu$_3$(OH)$_6$Br$_3$ were well refined by the cif file of its chloride analogues, indicating that the structure is the same as their chloride analogues LnCu$_3$(OH)$_6$Cl$_3$. The magnetic susceptibilities of LnCu$_3$(OH)$_6$Br$_3$ show a rapid increase around 16 K, where the specific heat displays a shoulder-like anomaly, which is attributed to the canted antiferromagnetic ordering of kagomé-Cu^{2+} spins. The low-T specific heat of NdCu$_3$(OH)$_6$Br$_3$ and SmCu$_3$(OH)$_6$Br$_3$ shows the typical Schottky anomaly. Moreover, the low-T magnetic susceptibilities of LnCu$_3$(OH)$_6$Br$_3$ show negative magnetization behaviors originating from the competition between Cu^{2+} and

†Corresponding author. E-mail: liqj@ahu.edu.cn
‡Corresponding author. E-mail: xfsun@ustc.edu.cn

© 2023 Chinese Physical Society and IOP Publishing Ltd

Ln^{3+} moments. Thus, the ground state of LnCu$_3$(OH)$_6$Br$_3$ displays a coexistence of magnetic ordering and exotic magnetic ground states due to the different Ln^{3+} ions.

2. Experiments

LnCu$_3$(OH)$_6$Br$_3$ (Ln = Nd, Sm, and Eu) single crystals were grown using the hydrothermal method. 5 mmol Cu(NO$_3$)$_2$·3H$_2$O (99.99%), 10.0 mmol Ln(NO$_3$)$_3$·6H$_2$O (Ln = Nd, Sm, and Eu) (99.99%) and 27.5 mmol KBr (99.0%), with the molar ratio Cu:Ln:Br=1:2:5.5, were mixed together with 2 mL deionized water. The mixtures were transferred to a stainless steel autoclave lined with teflon and heated to 230 °C for 3 days and then slowly cooled down to room temperature at a rate of 2 °C/h. The synthetic product was ultrasonically washed in water to remove impurities attached on the crystal surface. A large number of trial synthesis experiments showed that the best single crystals can be synthesized with the ratio of Cu:Ln:Br=1:2:5.5. In addition, KBr (99.0%) and Cu(NO$_3$)$_2$·3H$_2$O (99.99%) are the best bromine and copper sources for the crystal growth of LnCu$_3$(OH)$_6$Br$_3$. Other chemical reagents such as NaBr and CuC$_2$O$_4$ can lead to the formation of Cu$_2$(OH)$_3$Br single crystals and blue needle-like impurities. The crystal structures of LnCu$_3$(OH)$_6$Br$_3$ were checked by powder XRD at room temperature, with grounding some pieces of crystals into powder. The refinements of the crystal structure were performed by using the relative Rietveld powder diffraction profile fitting software FullProf. Magnetic susceptibility and magnetization were measured using a SQUID-VSM (Quantum Design). The specific heat was measured from 50 K to 2 K with a physical property measurement system (PPMS, Quantum Design).

3. Results and discussion

3.1. Crystal structure

Figure 1 shows the powder XRD patterns of LnCu$_3$(OH)$_6$Br$_3$ (Ln = Nd, Sm, and Eu) at room temperature. The refinements of the crystal structure of LnCu$_3$(OH)$_6$Br$_3$ are respectively compared to the cif files of its chloride analogues LnCu$_3$(OH)$_6$Cl$_3$ (Ln = Nd, Sm, and Eu). As shown in Fig. 1, the diffraction data could be well fitted to a Kapellasite type structure with space group $P\bar{3}m1$ (No. 164), and the well-refined results suggest that our crystals are of single phase. The unit cell parameters are $a = b = 6.8823(1)$ Å and $c = 5.8760(1)$ Å for NdCu$_3$(OH)$_6$Br$_3$, $a = b = 6.8522(1)$ Å and $c = 5.8717(1)$ Å for SmCu$_3$(OH)$_6$Br$_3$, $a = b = 6.8318(2)$ Å and $c = 5.8673(1)$ Å for EuCu$_3$(OH)$_6$Br$_3$. As shown in Table 1, the lattice parameters obtained by the Rietveld refinements decrease gradually with the decrease of the rare-earth ionic radius. The transparent and dark green LnCu$_3$(OH)$_6$Br$_3$ single crystals with hexagonal flake morphology (with size of ~ 1 mm and thickness of ~ 1 mm) are shown in the insets of Fig. 1.

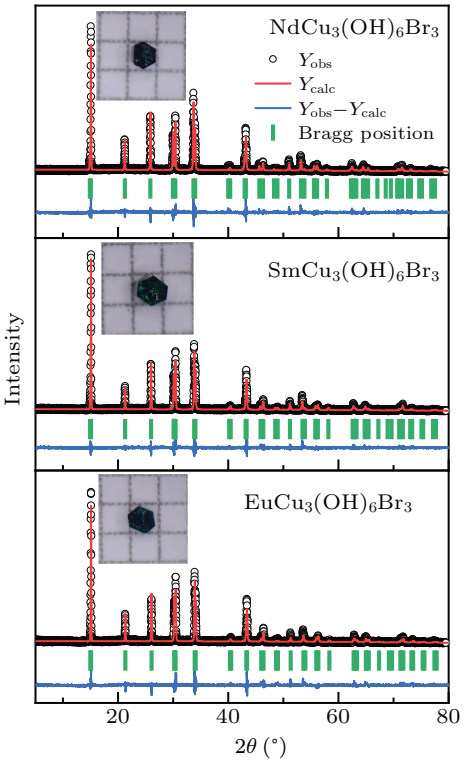


Fig. 1. Rietveld refinements of powder XRD data for LnCu$_3$(OH)$_6$Br$_3$ (Ln = Nd, Sm, and Eu). Experimental and calculated XRD patterns are all displayed. The vertical bars represent the expected Bragg reflection positions. The insets show photos of single crystals.

Table 1. The lattice parameters and magnetic parameters fitted by Curie–Weiss formula of LnCu$_3$(OH)$_6$Br$_3$ (Ln = Nd, Sm, and Eu).

	NdCu$_3$(OH)$_6$Br$_3$	SmCu$_3$(OH)$_6$Br$_3$	EuCu$_3$(OH)$_6$Br$_3$
$a = b$ (Å)	6.8823(1)	6.8522(1)	6.8318(2)
c (Å)	5.8760(1)	5.8717(1)	5.8673(1)
θ_{CW} (K)	–52.7	–257.5	–469.6
μ_{eff} (μ_B)	5.49	4.27	10.73

3.2. Magnetic properties

Figure 2 shows the zero-field-cooling magnetic susceptibility of LnCu$_3$(OH)$_6$Br$_3$ (Ln = Nd, Sm, and Eu) single crystals measured under 0.1 T with magnetic field along the kagomé plane and in the temperature range from 2 K to 300 K. All the magnetic susceptibilities present paramagnetic behavior at high temperatures, accompanied with a sharp increase with lowering temperature down to 16 K. As reported in LnCu$_3$(OH)$_6$Cl$_3$ (Ln = Nd, Sm, Eu, Gd, Tb, and Dy) previously,[22,23] such a rapid rise of magnetic susceptibilities is likely associated with the canted antiferromagnetic ordering of Cu^{2+} in the kagomé plane. Moreover, a similar transition in magnetic susceptibility of YCu$_3$(OH)$_6$Cl$_3$ was also observed and was attributed to the negative-vector-chirality 120° magnetic structure verified from the neutron scattering.[14] However, the sharp upturn behavior of magnetic susceptibility is not completely consistent with previous reports in YCu$_3$(OH)$_6$Br$_2$[Br$_x$(OH)$_{1-x}$] with different x, which

might be related to the content of bromine ions.[17,19] It is notable that for different Ln^{3+} (Ln = Nd, Sm, and Eu) ions, the magnetic susceptibilities behave differently at lower temperatures. The magnetic susceptibility of $NdCu_3(OH)_6Br_3$ increases rapidly and shows a shoulder-like feature around 10 K, which is likely another magnetic transition. The magnetic susceptibility of $SmCu_3(OH)_6Br_3$ shows a broad peak at 8 K, suggesting that a short-range antiferromagnetic ordering might be formed.[21] The magnetic susceptibility of $EuCu_3(OH)_6Br_3$ displays a platform around 8 K.[22]

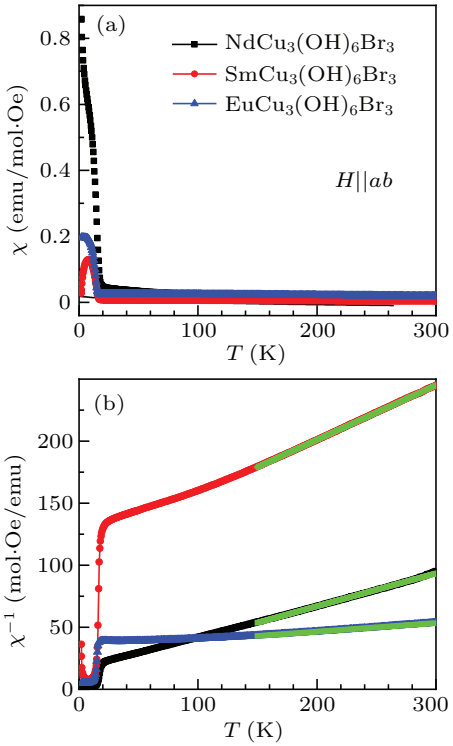


Fig. 2. (a) Magnetic susceptibility χ of $Ln Cu_3(OH)_6Br_3$ (Ln = Nd, Sm, and Eu) single crystals under 0.1 T magnetic field parallel to the kagomé plane. (b) Temperature dependencies of the inverse magnetic susceptibilities $1/\chi$. The green lines are the fitting of the high-T data by using the Curie–Weiss formula.

As shown in Fig. 2(b), the high-temperature (above 150 K) magnetic susceptibilities are well fitted by using the Curie–Weiss formula $\chi = C/(T - \theta_{CW})$, where C is the Curie constant and θ_{CW} is the Curie–Weiss temperature, with $\theta_{CW} = -52.7$ K, -257.5 K and -469.6 K for $NdCu_3(OH)_6Br_3$, $SmCu_3(OH)_6Br_3$ and $EuCu_3(OH)_6Br_3$, respectively. The large negative θ_{CW} values imply strong antiferromagnetic coupling in the Kapellasite $Ln Cu_3(OH)_6Br_3$. Using the formula $f = |\theta/T_N|$ and $T_N \sim 16$ K, the frustration parameters f are 3.51, 17.17 and 32.39 for $NdCu_3(OH)_6Br_3$, $SmCu_3(OH)_6Br_3$ and $EuCu_3(OH)_6Br_3$, respectively. These demonstrate that $Ln Cu_3(OH)_6Br_3$ have strong spin frustration effect. It is worth noting that the magnetic properties of $Ln Cu_3(OH)_6Br_3$ below $T_N = 16$ K are complex due to the introduce of Ln^{3+} ions, compared to $YCu_3(OH)_6Cl_3$ and $YCu_3(OH)_6Br_2[Br_x(OH)_{1-x}]$.[15,17]

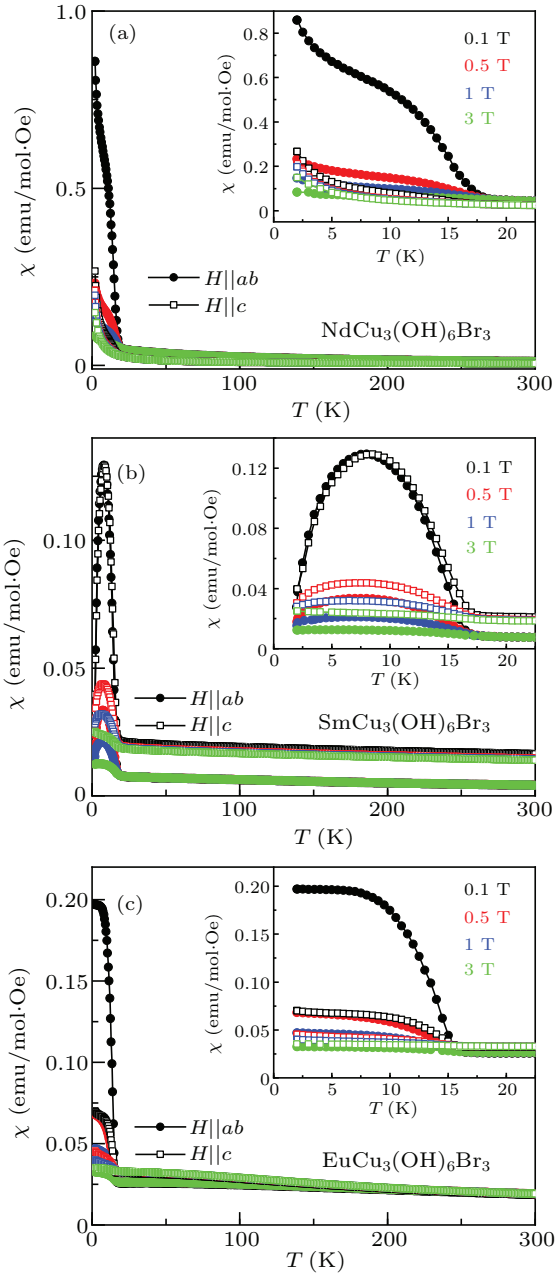


Fig. 3. Magnetic susceptibilities of $Ln Cu_3(OH)_6Br_3$ (Ln = Nd, Sm, and Eu) single crystals under different magnetic fields along the kagomé plane and the c axis. Insets are the zoom-in data at low temperatures.

Figure 3 shows more magnetic susceptibility data under different magnetic fields applied along the kagomé plane and the c axis. All the data were measured after zero-field cooling. First of all, the magnetic susceptibility is suppressed significantly with increasing magnetic field, while the canted antiferromagnetic ordering of Cu^{2+} ions still exists. Although the magnetic susceptibility is suppressed, the low-T behaviors, such as the shoulder-like feature around 10 K of $NdCu_3(OH)_6Br_3$, the broad peak at 8 K of $SmCu_3(OH)_6Br_3$ and the magnetic platform at 8 K of $EuCu_3(OH)_6Br_3$, still exist in magnetic fields up to 3 T. In addition, there is strong magnetic anisotropy for $Ln Cu_3(OH)_6Br_3$ (Ln = Nd and Eu) compounds at low magnetic fields, while there is weak magnetic anisotropy for $SmCu_3(OH)_6Br_3$.

To further characterize the magnetic properties, the magnetization of LnCu$_3$(OH)$_6$Br$_3$ (Ln = Nd, Sm, and Eu) single crystals was measured by applying the magnetic field along the kagmoé plane and the c axis, as shown in Fig. 4. At 2 K, the magnetization saturation of NdCu$_3$(OH)$_6$Br$_3$ is not achieved at 7 T with magnetic field along the kagomé plane, which is different from the c-axis results. In addition, under high magnetic fields, LnCu$_3$(OH)$_6$Br$_3$ (Ln = Sm and Eu) exhibit a linear field-dependence up to 7 T in both field directions. Using the above obtained parameters C and the formula $\mu_{\rm eff} = \sqrt{(3k_{\rm B}C/N_{\rm A})}$ ($k_{\rm B}$ is the Boltzmann constant, $N_{\rm A}$ is the Avogadro number), we estimated the effective magnetic moments of LnCu$_3$(OH)$_6$Br$_3$, which are 5.49$\mu_{\rm B}$, 4.27$\mu_{\rm B}$ and 10.74$\mu_{\rm B}$ for Ln = Nd, Sm, and Eu, respectively. For LnCu$_3$(OH)$_6$Br$_3$, the theoretical effective magnetic moments are 4.70$\mu_{\rm B}$, 3.11$\mu_{\rm B}$ and 3.00$\mu_{\rm B}$, which were calculated by formula $\mu_{\rm eff} = \sqrt{(3\mu^2_{\rm Cu^{2+}} + \mu^2_{Ln^{3+}})}$, where $\mu^{2+}_{\rm Cu} = 1.73\mu_{\rm B}$, $\mu^{3+}_{\rm Nd} = 3.62\mu_{\rm B}$, $\mu^{3+}_{\rm Sm} = 0.84\mu_{\rm B}$, $\mu^{3+}_{\rm Eu} = 0$. Experimental and theoretical effective magnetic moments have significant differences, suggesting that not all Ln^{3+} ions are at the ground state.[24] For NdCu$_3$(OH)$_6$Br$_3$, it is found that the effective magnetic moments of the experimental and theoretical results have little difference, while the discrepancy for LnCu$_3$(OH)$_6$Br$_3$ (Ln = Sm and Eu) means that not all Sm^{3+} and Eu^{3+} are at ground state due to spin–orbit coupling interactions. This is the main reason why we just observe the linear magnetization behaviors with magnetic fields up to 7 T in the case of Ln = Sm and Eu.[21,22,24]

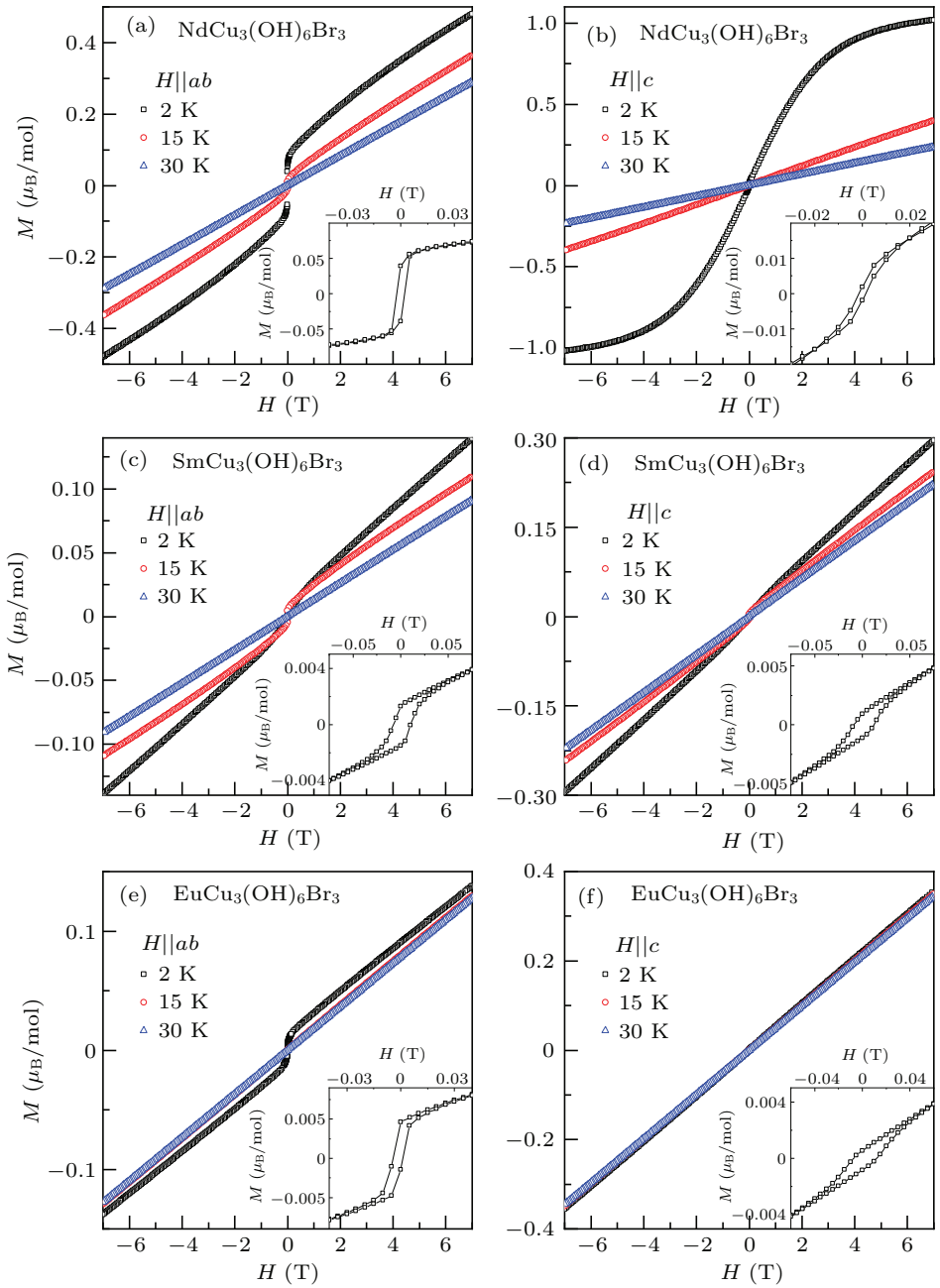


Fig. 4. Low-temperature magnetization of LnCu$_3$(OH)$_6$Br$_3$ (Ln = Nd, Sm, and Eu) for magnetic fields along the kagomé plane and the c axis. Insets are the low-field data at 2 K.

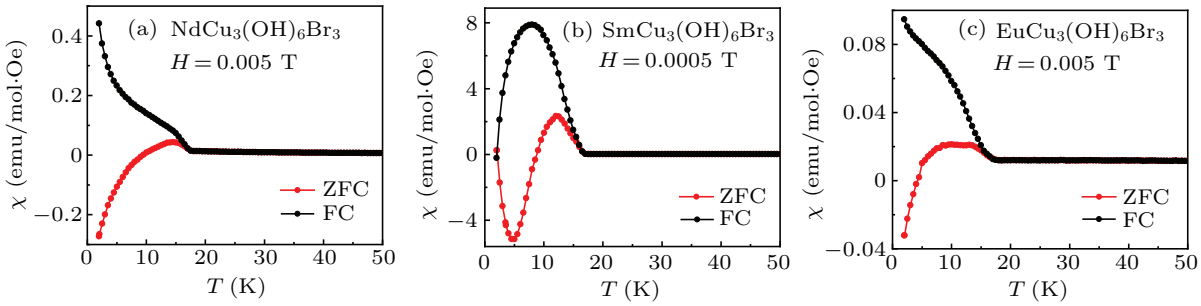


Fig. 5. Zero field-cooling (ZFC) and field-cooling (FC) magnetic susceptibilities of LnCu$_3$(OH)$_6$Br$_3$ (Ln = Nd, Sm, and Eu) single crystals under the c-axis magnetic field of 50 Oe, 5 Oe, and 50 Oe, respectively.

Moreover, the magnetization curves of LnCu$_3$(OH)$_6$Br$_3$ at 2 K display remarkable upturn at low filed, especially for the magnetic field along the kagmoé plane. Also, at 2 K the magnetization curves have a small but well defined hysteresis with magnetic field parallel to both directions, as shown in the insets of Fig. 4. It is further verified that LnCu$_3$(OH)$_6$Br$_3$ has weak ferromagnetic contribution arising from spin canting of Cu^{2+} ions because of the Dzyaloshinskii–Moriya (DM) interaction at low temperatures.[21,22,25,26]

In order to comprehensively investigate the ground state magnetic properties, we measured the zero-field-cooling (ZFC) and field-cooling (FC) magnetic susceptibilities of LnCu$_3$(OH)$_6$Br$_3$ at low temperatures. As shown in Fig. 5, with decreasing temperature, the ZFC and FC magnetic susceptibilities of LnCu$_3$(OH)$_6$Br$_3$ diverge near 16 K, which indicates the ferromagnetic contributions due to the canted antiferromagnetic coupling of Cu^{2+} in the kagomé plane. It is worth noting that the ZFC curves of LnCu$_3$(OH)$_6$Br$_3$ all show the negative magnetization at lower temperatures for weak magnetic fields. The negative magnetization behavior was also reported in LnCu$_3$(OH)$_6$Cl$_3$ (Ln = Nd, Sm, and Eu) previously.[21,22] Undoubtedly, it is attributed to the competing of the magnetic interactions between Ln^{3+} and Cu^{2+} magnetic sublattices. It is known that the magnetic sublattices of Cu^{2+} and Ln^{3+} in LnCu$_3$(OH)$_6$Cl$_3$ can couple antiferromagnetically due to the internal field of Cu^{2+} ions, that is, the Ln^{3+} paramagnetic moments are polarized antiparallel to the ferromagnetic moments of canted Cu^{2+} spins. Once the moments of the Ln^{3+} sublattice overcomes the Cu^{2+} moments, the total magnetization becomes negative.[27–30] As can be seen in Fig. 3, low-T magnetic properties are greatly affected by the magnetism of Ln^{3+} ions, compared to its chloride analogues YCu$_3$(OH)$_6$Cl$_3$ and YCu$_3$(OH)$_6$Br$_2$[Br$_x$(OH)$_{1-x}$].[13,17]

3.3. Specific heat

Figure 6 shows the specific heat of LnCu$_3$(OH)$_6$Br$_3$ single crystals at 2 K to 50 K with magnetic fields perpendicular to the kagomé plane. The zero-field specific heat displays a shoulder-like anomaly near T_N = 16 K, which is not affected by the applied magnetic fields up to 10 T. This is in consistent with the unchanged upturn of the magnetic susceptibility at ∼ 16 K under different magnetic fields, as shown in Fig. 3. As mentioned in previous report,[15] although this signature is different from the typical λ-type anomaly of specific heat at the Néel transition, our results support that the magnetic transition observed in magnetic susceptibility and specific heat is intrinsic. It is strongly suggested that the magnetic ordering could be attributed to the coupled Cu^{2+} spins within the kagomé plane.

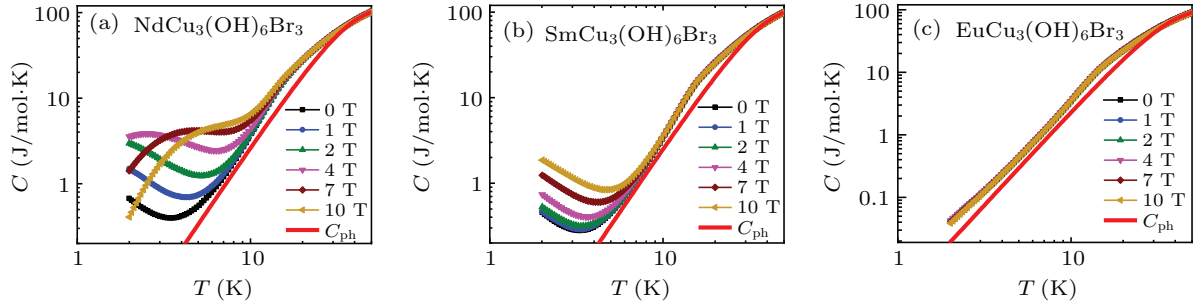


Fig. 6. Temperature dependencies of the specific heat of LnCu$_3$(OH)$_6$Br$_3$ (Ln = Nd, Sm, and Eu) single crystals under different magnetic fields perpendicular to the kagomé plane. The red lines represent the phonon contribution.

Meanwhile, the low-T specific heat shows more features. In order to obtain the magnetic contribution to the specific heat, the phononic specific heat is estimated by fitting the high-T data in zero field using the Debye formula $C_{ph} = \alpha T^3 + \beta T^5 + \gamma T^7$, as shown by the solid lines in Fig. 6. For NdCu$_3$(OH)$_6$Br$_3$, the zero-field specific heat develops an upturn at temperatures below 3.5 K and a broad peak appears near 2.5 K at 4 T. The position of this peak gradually moves

to higher temperatures with further increasing field, which can be interpreted as a characteristic Schottky anomaly related to the magnetic moment of the Nd^{3+} ion with the crystal electric field effect.[24,31] The specific heat of $SmCu_3(OH)_6Br_3$ also shows a low-T upturn that is more significant with increasing field. It might also be the Schottky anomaly caused by the crystal field levels of the Sm^{3+} ions.[24] In contrast, there is no low-T upturn in $EuCu_3(OH)_6Br_3$ with the magnetic fields up to 10 T, which is similar to its chloride analogues $EuCu_3(OH)_6Cl_3$.[22] Combined with the linear $M(H)$ of $EuCu_3(OH)_6Cl_3$ under high magnetic field, it is suggested that the magnetic field of 10 T is not sufficient to dominate the magnetic coupling of Eu^{3+} ions, where the energy splitting between the ground state and excited state is nearly 300 K due to the strong spin–orbit coupling of magnetic moment Eu^{3+} ions.

4. Discussion and conclusion

In summary, we have synthesized a series of $Ln Cu_3(OH)_6Br_3$ (Ln = Nd, Sm, and Eu) single crystals by the hydrothermal method. The Curie–Weiss fitting of magnetic susceptibilities reveals the existence of strong antiferromagnetic coupling in these systems. Magnetic measurements show that $Ln Cu_3(OH)_6Br_3$ have antiferromagnetic ordering transition near 16 K with strong spin frustration. The hysteresis in $M(H)$ curve at low temperatures indicates that $Ln Cu_3(OH)_6Br_3$ have weak ferromagnetism from canted antiferromagnetic couplings of kagomé Cu^{2+}. In the specific heat data, the shoulder-like anomalies of $Ln Cu_3(OH)_6Br_3$ are consistent with the rapid increase of the magnetic susceptibility. The typical Schottky phenomenon and negative magnetization behavior are attributed to the effect of Ln^{3+} ions on the low-T magnetic properties. Therefore, the $Ln Cu_3(OH)_6Br_3$ compounds feature strong magnetic frustration as well as canted antiferromagnetic ordering, and the magnetic contribution of Ln^{3+} ions on magnetic ground state cannot be neglected at low temperatures.

Acknowledgements

Project supported by the Natural Science Foundation of Anhui Province, China (Grant Nos. 2108085MA16 and 2108085QA22), the Key Project of Anhui Provincial Department of Education (Grant No. KJ2020A0013), the Key Project of the Foundation of Anhui Education Committee, China (Grant No. 2022AH050066), and the National Natural Science Foundation of China (Grant Nos. U1832209, 11874336, 12274338, 12104010, 12104011, 52102333, and 12004003).

References

[1] Balents L 2010 *Nature* **464** 199
[2] Gen M and Suwa H 2022 *Phys. Rev. B* **105** 174424
[3] Balz C, Lake B, Reuther J, Luetkens H, Schönemann R, Herrmannsdörfer T, Singh Y, Nazmul Islam A T M, Wheeler E M, Rodriguez Rivera Jose A, Guidi T, Simeoni Giovanna G, Baines C and Ryll H 2016 *Nat. Phys.* **12** 942
[4] Mei J W, Chen J Y, He H and Wen X G 2017 *Phys. Rev. B* **95** 235107
[5] Arh T, Gomilšek M, Prelovšek P, Pregelj M, Klanjšek M, Ozarowski A, Clark S J, Lancaster T, Sun W, Mi J X and Zorko A 2020 *Phys. Rev. Lett.* **125** 027203
[6] Paddison J A M, Daum M, Dun Z L, Ehlers G, Liu Y H, Stone M B, Zhou H D and Mourigal M 2017 *Nat. Phys.* **13** 117
[7] Yan S, Huse D A and White S R 2011 *Science* **332** 1173
[8] Fu M, Imai T, Han T H and Lee Y S 2015 *Science* **350** 655
[9] Helton J S, Matan K, Shores M P, Nytko E A, Bartlett B M, Yoshida Y, Takano Y, Suslov A, Qiu Y, Chung J H, Nocera D G and Lee Y S 2007 *Phys. Rev. Lett.* **98** 107204
[10] Khuntia P, Velazquez M, Barthélemy Q, Bert F, Kermarrec E, Legros A, Bernu B, Messio L, Zorko A and Mendels P 2020 *Nat. Phys.* **16** 469
[11] Lu F, Yuan L, Zhang J, Li B, Luo Y and Li Y 2022 *Commun. Phys.* **5** 272
[12] Bert F, Olariu A, Zorko A, Mendels P, Trombe J C, Duc F, Vries M A d, Harrison A, Hillier A D, Lord J, Amato A and Baines C 2009 *J. Phys.: Conf. Ser.* **145** 012004
[13] Sun W, Huang Y X, Nokhrin S, Pan Y and Mi J X 2016 *J. Mater. Chem. C* **4** 8772
[14] Zorko A, Pregelj M, Gomilšek M, Klanjšek M, Zaharko O, Sun W and Mi J X 2019 *Phys. Rev. B* **100** 144420
[15] Zorko A, Pregelj M, Klanjšek M, Gomilšek M, Jagličić Z, Lord J S, Verezhak J A T, Shang T, Sun W and Mi J X 2019 *Phys. Rev. B* **99** 214441
[16] Barthélemy Q, Puphal P, Zoch K M, Krellner C, Luetkens H, Baines C, Sheptyakov D, Kermarrec E, Mendels P and Bert F 2019 *Phys. Rev. Mater.* **3** 074401
[17] Chen X H, Huang Y X, Pan Y and Mi J X 2020 *J. Magn. Magn. Mater.* **512** 167066
[18] Zeng Z Y, Ma X Y, Wu S, Li H F, Tao Z, Lu X Y, Chen X H, Mi J X, Song S J, Cao G H, Che G W, Li K, Li G, Luo H Q, Meng Z Y and Li S L 2022 *Phys. Rev. B* **105** L121109
[19] Liu J, Yuan L, Li X, Li B, Zhao K, Liao H and Li Y 2022 *Phys. Rev. B* **105** 024418
[20] Hong X, Behnami M, Yuan L, Li B, Brenig W, Büchner B, Li Y and Hess C 2022 *Phys. Rev. B* **106** L220406
[21] Sun W, Huang Y X, Pan Y and Mi J X 2017 *Dalton Trans.* **46** 9535
[22] Puphal P, Zoch K M, Désor J, Bolte M and Krellner C 2018 *Phys. Rev. Mater.* **2** 063402
[23] Fu Y, Huang L, Zhou X, Chen J, Zhang X, Chen P, Wang S, Liu C, Yu D, Li H F, Wang L and Mei J W 2021 *Chin. Phys. B* **30** 100601
[24] Matsuhira K, Wakeshima M, Hinatsu Y and Takagi S 2011 *J. Phys. Soc. Jpn.* **80** 094701
[25] Rousochatzakis I, Manmana S R, Läuchli A M, Normand B and Mila F 2009 *Phys. Rev. B* **79** 214415
[26] Lee C Y, Normand B and Kao Y J 2018 *Phys. Rev. B* **98** 224414
[27] Kumar A and Yusuf S M 2015 *Phys. Rep.* **556** 1
[28] Wang Y, Ni S, Zhang H, Wang H, Su K, Yang D, Huang S, Huo D and Tan W 2022 *Appl. Phys. A* **128** 839
[29] Yang A M, Sheng Y H, Farid M A, Zhang H, Lin X H, Li G B, Liu L J, Liao F H and Lin J H 2016 *RSC Adv.* **6** 13928
[30] Kumar P, Kumar R, Pandey S, Suresh K G and Nigam A K 2014 *Physica B* **448** 6
[31] Li Q J, Zhao Z Y, Zhou H D, Ke W P, Wang X M, Fan C, Liu X G, Chen L M, Zhao X and Sun X F 2012 *Phys. Rev. B* **85** 174438